Food Hydrocolloids 121 (2021) 106982

Contents lists available at ScienceDirect

Food Hydrocolloids

journal homepage: www.elsevier.com/locate/foodhyd

Effects of aging on the shelf life and viscoelasticity of gellan gum microcapsules

Yun-Han Huang [a], Xiran Li [b], Mariano Michelon [c], Bruna C. Leopercio [d], Marcio S. Carvalho [d], John M. Frostad [a,b,*]

[a] Chemical and Biological Engineering, University of British Columbia, Canada
[b] Food Science, University of British Columbia, Canada
[c] School of Chemistry and Food Engineering, Federal University of Rio Grande, Brazil
[d] Department of Mechanical Engineering, Pontifical Catholic University of Rio de Janeiro, Brazil

ARTICLE INFO

Keywords:
Core-shell capsule
Microcapsule
Gellan gum
Aging
Shelf life
Viscoelasticity

ABSTRACT

Microcapsules are of great interest for applications such as targeted drug delivery and encapsulation of functional food ingredients. While it is intuitive that such products age over time and have a finite shelf life, there are few studies on how the properties of microcapsules change with aging. Here, we examine the aging of edible, gellan gum microcapsules both qualitatively and quantitatively. We found that changes occur in the structure, color, stability, and even the density of individual microcapsules. Further, we performed extremely precise measurements of the rheological properties of the microcapsules using a cantilevered-capillary force apparatus and showed the necessity of method development in order to correctly interpret the data and carry out similar studies in the future. For the aged microcapsules, we observed a transformation from relatively soft and purely elastic to increasingly more stiff and viscoelastic under small deformations, as well as plastically deforming at larger deformations. Ultimately, the microcapsules were found to completely lose their integrity by spontaneously shedding the outer shell and aggregating.

1. Introduction

In general terms, microcapsules are micro-scaled spheres that are composed of more than one type of material. Therefore, the term microcapsule can encompass everything from geometrically simple, spherical particles with a liquid core and solid shell, to particles with multilayer-shell structures, to heterogeneously distributed solid domains embedded within a solid microsphere (Biviano et al., 2021; Huang et al., 2019; Liu et al., 2005; Ozkan et al., 2019; Paulo & Santos, 2017). In this study, we focus on the type of microcapsules that are composed of a single liquid core surrounded by a thin layer (but with finite thickness) of soft, shell material. Hereafter in this manuscript, we refer to these as "core-shell microcapsules" or simply "microcapsules" for brevity.

Microcapsules have a wide range of applications and their mechanical properties often play an important role. For instance, the ability to resist stress is critical for microcapsules that undergo deformation in their applications, such as drug delivery vehicles that must pass through needles and narrow blood capillaries, or edible microcapsules that must survive processing and mastication. In both cases it is desired to maintain a sustained release of their contents, so a premature rupture would be a negative outcome (Liu et al., 2005; Zhao et al., 2007). As another example, Caruso et al. designed double-walled microcapsules with improved mechanical properties use in self-healing polymers (Caruso et al., 2010).

Researchers have developed various methods and theories to study the stiffness of coreshell microcapsules. For example, studies have utilized an atomic force microscope (Chen et al., 2012; Mercadé-Prieto & Zhang, 2012; Sliwka, 1975; Utada et al., 2005; Lulevich, 2003), micro-manipulation devices (Ashkin et al., 1987; Zhang, 1999), and optical tweezers (Neubauer et al., 2014; Suresh et al., 2005; Tan et al., 2010) to measure the force-displacement relationship of a microcapsule. A detailed discussion of the various methods and their advantages and limitations can be found in the following review papers: (Fery & Weinkamer, 2007; Mercadé-Prieto & Zhang, 2012). In our own recent work, we demonstrated the use of a cantilevered-capillary force apparatus (CCFA) to obtain elastic moduli of edible microcapsules (Huang et al., 2021).

* Corresponding author. Chemical and Biological Engineering, University of British Columbia, Canada.
E-mail address: john.frostad@ubc.ca (J.M. Frostad).

https://doi.org/10.1016/j.foodhyd.2021.106982
Received 6 February 2021; Received in revised form 20 May 2021; Accepted 21 June 2021
Available online 29 June 2021

Besides the elasticity of the microcapsules, viscoelasticity can also play an important role in affecting their capabilities. For example, the relaxation time of a microcapsule determines the time required to restore its original shape after a deformation. This can impact the performance in self-healing materials applications (Han et al., 2019), or whether they can survive an imposed stress (Kim et al., 2008). Furthermore, if the viscoelastic properties are frequency-dependent, then the behaviors of the microcapsules may vary under different strain rates. Therefore, when designing the microcapsules, one will need to select suitable properties based on the dynamic conditions in the applications.

However, while the elasticity of microcapsules is usually characterized by compressing individual microcapsules, the rheology is more often measured on entire microcapsule suspensions (Borgogna et al., 2010; Wang et al., 2020) or the bulk shell materials alone (Verheyen et al., 2019). In these methods, the rheological properties of the microcapsules are either represented by the macroscopic view of the solutions or the properties of the same materials with a different geometry. Therefore, it may be difficult to quantify the actual amount of deformation the microcapsules undergo during the measurement and make it challenging to establish the relationship between microcapsule rheology and their performance.

In light of this, researchers have also attempted to employ single-capsule methods for characterizing rheology. For instance, Han et al. used an atomic force microscope (AFM) and a Voigt model with Maxwell elements to characterize urea-formaldehyde microcapsules (Han et al., 2019). Kim et al. used a microgripper and a Voigt model that is based on Tatara's theory to characterize hydrogel microcapsules for drug delivery applications (Kim et al., 2008). In these works, the rheological properties of the microcapsules are extracted through ramping or stress relaxation tests, and therefore they did not specifically study the frequency dependence of the viscoelasticity.

Only a few researchers (Biviano et al., 2021; Zhang et al., 2020) characterized the rheological properties by applying oscillating deformation. For shear deformation, a recent study examined dynamic modes of viscoelastic microcapsules in oscillating shear flow using the finite-element method (Zhang et al., 2020). Also, Biviano et al. treated an oil-in-water emulsion droplet as a "microcapsule," and used the Reissner model to obtain the complex dynamic moduli under uniaxial deformation (Biviano et al., 2021). In these studies, it is common to examine the stress-strain curves to qualitatively identify the presence of phenomena such as adhesion force (Sirghi, 2010) or molecular structuring within the material (Giménez-Ribes et al., 2020).

In terms of mechanical properties, aging of the material can directly affect the functionality of microcapsules and/or degrade their performance. Note that the term "aging" may refer to various concepts in different contexts. For instance, researchers have referred it to as a step of the fabrication process (Li et al., 2015) or to maintaining microcapsules under specific environmental conditions such as UV exposure (Luo et al., 2020) or in a nickel plating bath (Alexandridou, 1995). Here we refer to aging as the change in properties that occurs over time while in storage. Hence, in this context the speed or degree of aging is a measure of the shelf-life of the microcapsules.

In many applications, the role of the shell of the microcapsules is to isolate the core from the surrounding fluid and preserve its functionality. Therefore, researchers often use a change in core composition as an indicator of aging. One method is to measure the weight loss of microcapsules after different storage times (Alizadegan et al., 2017; Wang et al., 2011). However, under certain situations, the microcapsules may need to serve more complex purposes, such as withstanding deformation or maintaining sustained release of active ingredients (Liu et al., 2005; Zhao et al., 2007). In these scenarios, composition changes as an indicator of aging or functionality is not enough.

Since mechanical properties are critical in tailoring the properties of microcapsules, they may also serve as an indicator of aging. However, to our best knowledge, only Lulevich et al. correlated the mechanical properties of single microcapsules to their ages by showing that polyelectrolyte multilayer microcapsules soften as they age due to loss of water from inside the microcapsule (Lulevich et al., 2004). Therefore, there is a large knowledge gap related to the correlation between aging of microcapsules and their rheological properties.

In this work, we aim to provide new insights into the cause of aging and resulting changes in gellan gum microcapsules. In particular, we investigate whether it is possible to use rheological properties as an indicator of the aging of microcapsules. This is approached by dynamic uniaxial compression experiments on gellan gum microcapsules using a cantilevered capillary force apparatus (CCFA) (Frostad et al., 2013, 2016; Frostad, Collins, et al., 2014; Frostad et al., 2014). In order to perform this experiments, it was necessary to address some important practical considerations for making these measurements: backlash and loss of contact. We show how they can influence the interpretation of data and offer suggestions for how they might be dealt with.

2. Materials and methods

2.1. Gellan gum microcapsules

The core-shell microcapsules studied in this work are fabricated with a device composed of two coaxial cylindrical glass-capillaries. The microcapsule is formed by a three phase flow: inner phase (core material), middle phase (shell material), and a continuous phase. The inner phase flows through the injection capillary, while the middle and continuous phase flow in opposite directions through the gap between the two capillaries. By using this technique, the radius, shell thickness, and the composition of the resulting microcapsules are tunable. The complete details for the production method can be found in a previous publication (do Nascimento et al., 2017; Michelon et al., 2020).

For the microcapsules used in this research, the core is composed of sunflower oil with an orange food-grade dye, and the shell consists of a mixture of 0.5 wt% or 1 wt% low-acyl gellan gum Kelgogel® CG-LA (CP Kelco BrasilS/A, Brazil) and 2 wt% polyoxyethylene sorbitan monolaurate, Tween®20 (Sigma-Aldrich, USA), in ultrapure water with resistivity of 18.2 MΩ/cm (Direct-Q3 UV System, Millipore Co., USA). Table 1 lists the parameters of the various microcapsule sizes tested in this study.

2.2. Force-displacement measurements

A cantilevered-capillary force apparatus (CCFA) is used to measure the force-deformation relationship of the microcapsules (Frostad et al., 2013). Briefly, the tested microcapsule is held at the tip of a capillary that also measures the applied force while the microcapsule is compressed by a rigid plate. The detailed working mechanism along with a protocol of how to manipulate the sample is discussed in a previous paper (Huang et al., 2021).

Besides the static compression for obtaining the elastic modulus, a dynamic measurement (referred to as dynamic tests hereafter) is also done in this work. The dynamic tests were done by oscillating the position of the rigid plate and measuring the response of the force. From

Table 1
Summary of microcapsule parameters tested. The three-letter code indicates the size (small - S, medium - M, large - L), shell thickness (thin - t, thick - T), and weight percent of gellan gum in the shell material (0.5% - g, 1.0% - G).

Code	Diameter (μm)	Shell thickness (μm)	Gellan Gum (wt%)
Stg	110	6	0.5
Mtg	158	7	0.5
Ltg	206	7	0.5
MTg	160	12	0.5
LTG	197	13	1
LtG	189	5	1
MtG	158	7	1

these data the storage and loss moduli of the microcapsules can be obtained as discussed in section 3.5. In the dynamics tests, the time-dependent position $x(t)$ is given by:

$$x(t) = x_A \sin \omega t + x_0, \tag{1}$$

where x_0 is the initial deformation, x_A is the amplitude, and ω is the frequency. Note, that the time-dependent deformation is a slightly modified sinusoidal function as compared to the typical standard sine function used in shear rheometry. This is because a sinusoidal function contains both positive and negative parts, which means that a sample undergoing sinusoidal strain is stretched and compressed during the deformation. However, in this study the microcapsule is only compressed and not stretched.

In this study, we target the region of small deformation to match the assumption of linear viscoelasticity. Therefore, the deformation was set to oscillate between a minimum of 5% and a maximum of 10% compression. However, due to challenges in determining the precise point of compressive contact (as discussed in previous work (Huang et al., 2021)), the actual compression amounts varied somewhat from these set points.

2.3. Governing equation for CCFA

When making dynamic force measurements it is important to remember that the force measured by the cantilever is not necessarily equal to the force applied on the microcapsule. Instead, the governing equation for the motion of the tip of the cantilever capillary is given by the equation for a driven, harmonic oscillator:

$$m_{eff}\ddot{x} + b\dot{x} + kx = F(t). \tag{2}$$

Here x is the position of the tip of the cantilever, m_{eff} is the effective mass, b is the hydrodynamic drag coefficient, k is the spring constant, and $F(t)$ is the sum of all forces exerted on the capillary during the experiment.

By non-dimensionalizing, the left side of the equation can be written as:

$$\frac{m_{eff}}{kt_c^2}\ddot{\xi} + \frac{b}{kt_c}\dot{\xi} + \xi. \tag{3}$$

here ξ is the dimensionless displacement and t_c is the characteristic time of the motion. In the present experiments, t_c can be represented by the period of the oscillation which ranges from 10^{-1}–10^{2} s. The values of m_{eff}/k and b/k are $O(10^{-5})$ and $O(10^{-3})$. Therefore, the magnitudes of the inertial force and the drag force range from 10^{-9} to 10^{-3} and 10^{-5} to 10^{-2} respectively. This means that the signal from the CCFA is well-approximated by the Hooke's law component, and the contribution due to inertia and drag force can be neglected in the present work.

2.4. Capsule aging

Two types of aging of the microcapsules were carried out in this study. First, the entire batch of each microcapsule type was stored in a refrigerator in acetate buffer solution for a period of several months. The acetate buffer contained 0.03 M sodium acetate (Sigma-Aldrich) solution and 44 mM acetic acid (Fisher Scientific™) solution with a final pH between 4.5 ± 0.1. Second, individual microcapsules were isolated and monitored over a period of days at room temperature in the same solution. In one case, time-lapse imaging (at 2 min intervals) with a bright field microscope (Nikon Labophot-2) and a camera (iDS camera UI-3880LE) was used to visualize changes in the microcapsule.

As a comparison, we also characterized the elastic modulus of the aged gellan gum gel. The gellan gum solution consisted of a mixture of 0.5 wt% low-acyl gellan gum (Kelcogel CG-LA) and 2 wt% Tween 20 (Fisher Scientific). The solution was mixed at 80°C for 10 min under magnetic stirring, and 5 mM of calcium chloride dihydrate (VWR International) was added for the formation of the gel. The elastic moduli of fresh and aged (3 and 6 days) gellan gum gel were characterized with a TA.XTplus Texture Analyser (Texture Technologies Corp.).

3. Results and discussion

3.1. Overview of observations related to aging

As the gellan gum microcapsules aged, we observed several noteworthy changes. First, we observed an increase in their densities, causing them to sink to the bottom of the solution, while the fresh microcapsules stayed afloat in the solution (Fig. 1(a)). Besides the change in density, aggregation also occurred. These phenomena occurred relatively quickly (within 1–2 weeks) under room temperature, and happened more slowly when storing the microcapsules at 4°C. We also noticed that the speed of aging varies with the type of microcapsule. However, for the seven types of microcapsules studied in this work, we did not see a correlation between aging speed and the geometry or composition.

A second observation was that the aged microcapsules became more fragile. For instance, rupture was observed during the compression of an aged microcapsule (Fig. 1(a)). This is in contrast to fresh microcapsules that can withstand relatively large compression (as much has 40%) in a completely reversible manner (Huang et al., 2021).

Aside from rupturing, aged microcapsules also showed irreversible (plastic) deformation. As shown in Fig. 1(b), the point of contact during sequential compressions shifted after every compression. To quantify the irreversible deformation, we used the method utilized by Okwara et al. (2021) to characterize permanent plastic deformation of neurospheres. For the data in Fig. 1(b), about 3–4% of the applied deformation was irreversible in each run of the compression. The final compression shows an irreversible deformation of more than 10% of the microcapsule diameter, which is significant and cannot be neglected.

The final observation that we wish to describe is that the stiffness increases as the microcapsules age. Fig. 1(c) shows that the effective elastic modulus of three different microcapsules from the same batch (type: MTg) increased by nearly four orders of magnitude over a period of about 7 months. For these samples, the increasing modulus was accompanied by a darkening in the appearance. Taken together, all of these changes during aging will clearly have a large impact on their application in foods or other systems.

3.2. Influence of aging on stiffness

In order to provide a more quantitative characterization of the effect of aging on stiffness, we performed an "accelerated" aging test on a single microcapsule by maintaining it at room temperature (rather than in the refrigerator) for a week. The effective elastic modulus of the microcapsule is obtained once per day via the force-displacement curve using the linear Tatara model (Tatara, 1991; Tatara et al., 1991) as recommended in a previous study (Huang et al., 2021). Fig. 2(a) shows the force-displacement curves of the microcapsule on each day. Here we have defined the strain as the displacement divided by the diameter of the undeformed microcapsule.

Fig. 2(b) shows the relationship between the effective elastic modulus and the age of the microcapsule. Note that the age of the microcapsule is defined relative to the time it has been kept at room temperature. From these results we see that the effective modulus increased by a factor of 40 ($E_{7\text{days}} \approx 42E_{0\text{days}}$) during the 7 days of accelerated aging.

At the same time, we also observed irreversible deformation of the microcapsule as a result of the measurement itself. According to the images of the microcapsules shown in Fig. 2(c), the irreversibility is first noticeable after about 2 days of aging. After irreversible deformation has occurred, the initial shape of the microcapsule is no longer a perfect sphere.

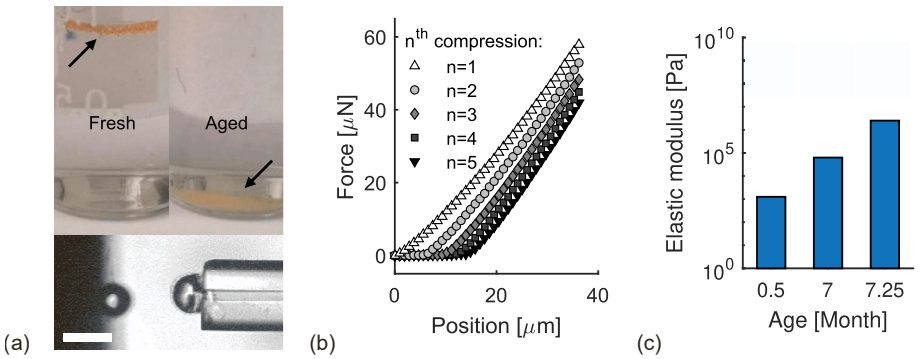

Fig. 1. (a) Images of fresh, aged, and ruptured (bottom) microcapsules. (b) Representative data of irreversible deformation of an aged microcapsule (capsule type: MTg). (c) Relationship between elastic moduli and storage time at 4 °C (capsule type: MTg).

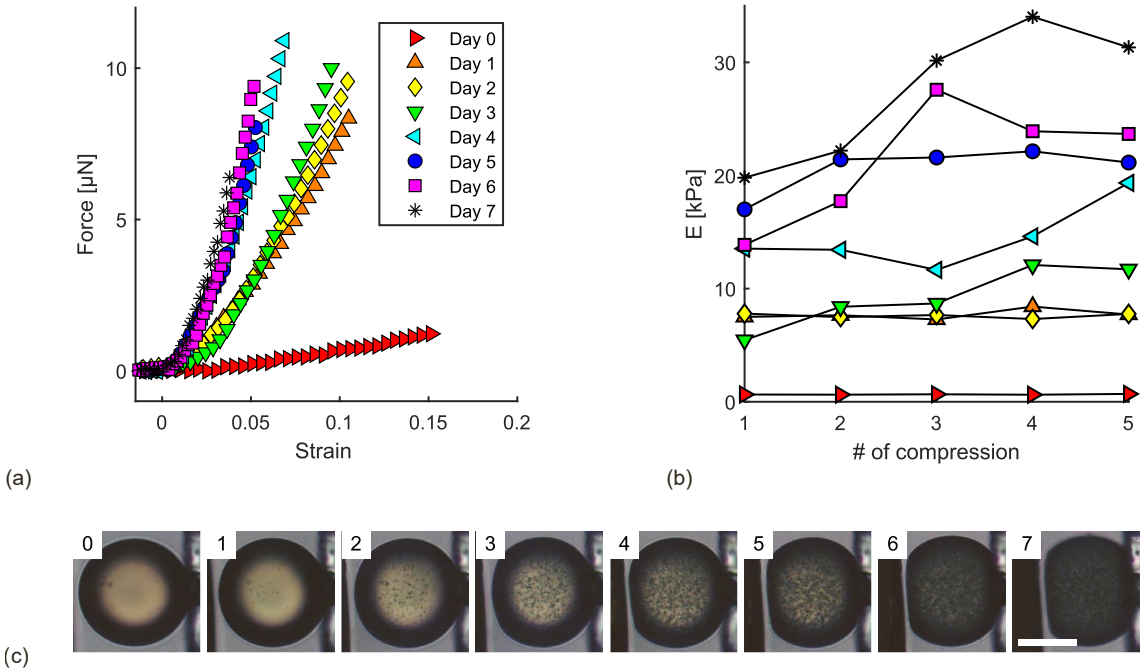

Fig. 2. (a) Force-strain curves of the microcapsule at different ages. (b) Elastic moduli of each compression at different ages. The lines are meant to guide the eye. (c) Images of the microcapsules at different ages. The number at the top right corner represent the age of the microcapsule (unit: days).

Therefore, the assumption of a spherical shape in the constitutive model is violated and the measured moduli are ill-defined, though still useful for comparison. We see this effect in Fig. 2(b) where for 0–2 days the moduli are fairly consistent from one compression to the next, while as the age increases, the variation in the moduli also increases with subsequent compressions.

In addition, by examining the images of the microcapsule through the 7 days of aging in Fig. 2(c), the appearance of the microcapsule became darker just as observed for microcapsules stored at 4°C over a period of months. Here speckles were observed to appear in the microcapsule as well. From these images it is not clear what structures in the microcapsule cause these speckles to appear or even if they are present in the core of the microcapsule, the shell, or both. To provide additional insight, we carried out time-lapse imaging on a microcapsule that did not undergo deformation. Those results are discussed in the next section.

We also characterized the elastic modulus of a bulk sample of fresh and aged gellan gum gel. Note that the elastic moduli of the gellan gum gel are different from the shell moduli we extracted in the previous study (Huang et al., 2020). This is due to the difference in the concentration of calcium ions, which can influence the elastic modulus of the gel significantly (Sworn & Kasapis, 1998). While preparing the microcapsules, calcium acetate was added to the sunflower oil phase. Therefore, there can be residual calcium ions in the core, and we were unable to know the actual amount of ions that participated in the formation of the gel. Interestingly, the moduli of the bulk gellan gum did not change significantly after stored under room temperature for seven days (fresh: 123 ± 11 kPa, 3 days: 137 ± 5 kPa, and 6 days: 125 ± 17 kPa). This suggests that the observed change in elastic modulus of the microcapsules is not due to changes in the shell material. Instead, it suggests that the composition of the core changed and we return to this point later on.

3.3. Spontaneous shedding of microcapsule shell

Time-lapse imaging of microcapsules at room temperature (accelerated aging) in a sealed microscopic vessel allow us to make a couple of additional observations related to aging. Fig. 3(a) shows micrographs of a microcapsule from the same batch (type: Ltg) as the microcapsule studied in the previous section. Note that, as before, the age of the microcapsule is defined relative to the time it has been stored at room temperature, i.e., since the beginning of the measurement. Again, the microcapsule becomes darker with age and appears speckled, though in this case there were already some speckles at the beginning of the

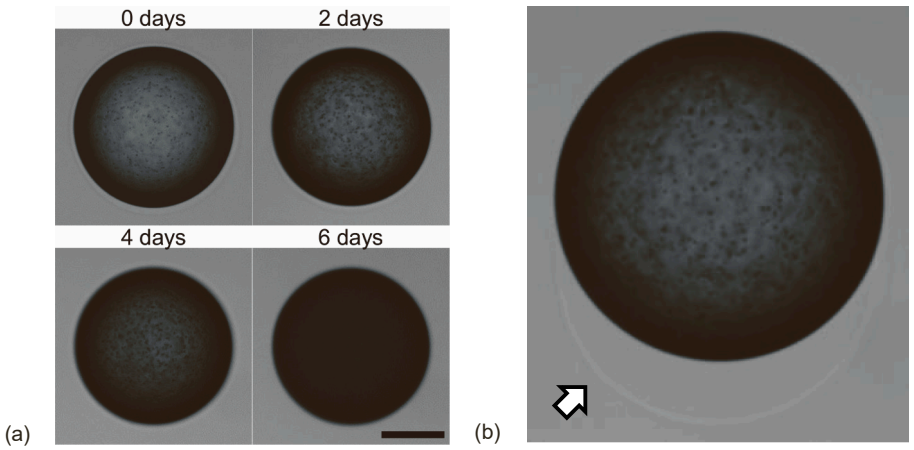

Fig. 3. (a) Images of the microcapsule (Ltg) at different ages. (b) An image showing the detachment of the shell (indicated by the arrow).

imaging. This is because the time-lapse imaging was conducted at a later date than the previous test and the microcapsules stored in the refrigerator had continued to age during the intervals between the two studies.

Interestingly, after about 48 h of aging we also observe a spontaneous separation of the shell of the microcapsule from the core of the microcapsule as shown in Fig. 3(b). The separation process took about 8 h and we noticed that the core of the microcapsule seems to be moving while the shell remains stationary. We speculate that this may be due to some amount of adhesion between the shell material and the glass, but do not have evidence to support this. In either case, this shedding of the shell material is likely to be the cause for the aggregation of the microcapsules that we observed in long-term storage.

By further examining the time-lapse video of the experiment (provided in the supplementary material), we also observe that the location of the speckles appear to be stationary within the microcapsule as it rotates. The speckles also remain in place after the shell has been shed from the core. This shows that the speckles and darkening occur within the core of the microcapsule independently of the shell material.

In terms of the driving force for the core-shell separation process, gellan gum is known to be permeable to water (Yang et al., 2013). This implies that when the microcapsules are submerged in ionic solutions, the osmotic pressure can result in them losing water content and shrinking. Another study reported that the volume of gellan gum gel increased when immersed in distilled water (Nitta, 2005). Therefore, one possible mechanism is that shrinkage of the shell material generated enough force to squeeze the core out of the shell. This speculation needs to be further tested since we did not observe significant volume changes in microcapsules or gellan gum gel.

Finally, we monitored the radius of the core of the microcapsule throughout the timelapse imaging. At the end of the test, the decrease of the radius is found to be approximately 2% of the initial radius (≈2 μm), which is close to the resolution of the image (2.7 pixel/μm). Therefore, our findings suggest that the radius of the microcapsule remained constant during the process of aging. Unfortunately, none of these observations offer additional insight into the reason for the change in *density* of the microcapsules.

3.4. Measurement of rheological properties

One of the advantages of using a CCFA to study these microcapsules is that it is possible to carry out detailed mechanical characterization. However, methods and models for such characterization of microcapsules are still in the early stages of development (Biviano et al., 2021; Zhang et al., 2020). Here we present some of the practical considerations one must account for in making these measurements (particularly dynamic measurements), as well as a description of the influence on the collected data. We also present dynamic measurements to give both qualitative and quantitative examples of the effects of aging on the mechanical properties of microcapsules.

3.4.1. Practical considerations: Backlash correction

During dynamic measurements, the direction of actuation changes periodically and therefore one must evaluate the influence of backlash on the deformation applied to the microcapsules. Backlash in the CCFA occurs due to imperfectly rigid connections between the rigid capillary and the piezoelectric actuator, which results in the programmed displacement not being equal to the actual displacement. The amount of backlash is quantified by running an oscillation test with the rigid capillary directly in contact with the cantilevered capillary. The result is a parallelogram, with the width of its bottom defined as the backlash length ΔL as shown in Fig. 4(a). The ΔL in this study is 2.50 ± 0.085 μm, and in many cases is not negligible compared to the amplitude of the oscillation.

Also, we want to point out that the initial position between the rigid capillary and the stage at the start of a measurement can also affect the backlash behavior. For example, if the rigid capillary was previously moving forward (prior to a given measurement), the capillary will move with the actuator as soon as the motion begins. On the other hand, if the previous motion was backward, then there will be a lag between the initial motion of the actuator and the capillary as the backlash distance is traversed. However, when the motion of the actuator is periodic (as in this study) the initial position only influences the beginning of the oscillation. Afterwards, the history of any motion prior to the experiment is erased.

Knowing that backlash is not negligible, we examine how it affects the force-displacement profile. Here we consider fabricated data — with and without backlash — for a sinusoidal compression of a microcapsule and plot it as a "Lissajous plot" to see the force-displacement profile. For a material that is purely elastic following Hooke's law (Fig. 4(b)) or following Hertz law (Fig. 4(d)), the observed relationship between force and the programmed displacement will show an artificial phase delay. Therefore, if one does not account for the backlash, then it is possible to falsely conclude that the material is viscoelastic.

Next we fabricated data for a material that is viscoelastic in Fig. 4(c) and (e) — the models used to generate this data are discussed in section 3.4.3. For a viscoelastic material, the force-displacement profile is expected to be a closed loop, but the backlash produces artificial "twists" in the data at both ends and a more narrow loop. Therefore, the artifacts in the data would be difficult to explain and the viscoelasticity would be underestimated. While these issues may be significant, it is worth noting that backlash correction can be done in post-processing of the data so the presence of backlash does not necessarily invalidate collected data.

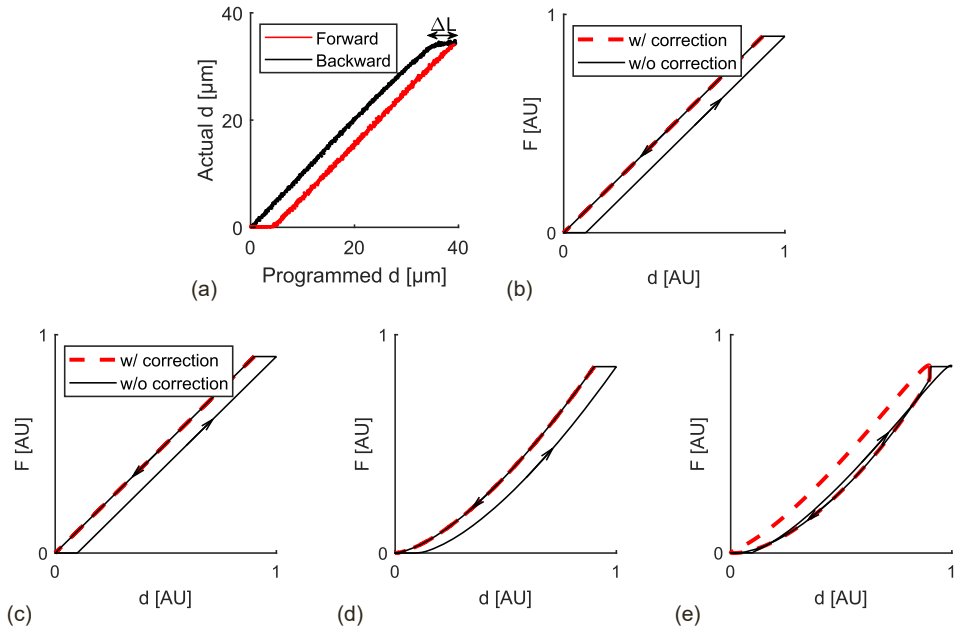

Fig. 4. (a) Relationship between programmed displacement and actual displacement measured by conducting the oscillation test with no specimen (rigid capillary directly compressing the cantilevered capillary). (b–e) Influence of backlash on the force-displacement curves of (b) purely elastic material with linear F-d relationship, (c) viscoelastic material with linear F-d relationship, (d) purely elastic sphere, and (e) viscoelastic sphere.

3.4.2. *Practical considerations: Loss of contact*

Because the microcapsules in these experiments are under compression, but not under tension, it is possible for loss of contact between the microcapsule and the compression plate to occur. Fig. 5 shows an example of this situation where the force is zero for a certain period of time, while the position of the rigid capillary continues oscillating. In Fig. 5(a) the out-of-contact portion of the curve falls between the points labeled B and C, and results in a horizontal portion of the force-displacement curve in Fig. 5(b).

Also, as one may notice, a portion of the force is negative in the region between B and C. As discussed before, the microcapsule should only be under compression, but negative forces indicate tensions. A negative force in this case can be caused by lubrication forces or adhesion forces between the microcapsule and the rigid capillary. In this study, we believe it is due to the lubrication force rather than adhesion, and this will be discussed further in section 3.5.

Here the reason for the loss of contact is the viscoelasticity of the microcapsule. If the microcapsule is fully elastic, as the rigid capillary retreats the microcapsule will deform instantaneously, and therefore the two objects will always be in contact. However, if the microcapsule is viscoelastic, the deformation will be delayed due to relaxation, which will result in a gap between the surface of the microcapsule and the rigid capillary. For this situation, the time spent of out of contact provides insight about the time scale of relaxation for the microcapsule. However, the stress and strain are not known when the capillary is not in contact with the microcapsule.

3.4.3. *Practical considerations: Availability of constitutive models*

Dynamic measurements are required for understanding the viscoelasticity of the microcapsules. However, in order for such measurements to be quantitative we require an appropriate constitutive model for the material and geometry. Here we present one model that might be used for this purpose. However, we note that there is not a consensus in the literature for which, if any, of the available models are correct.

In the case of a spherical microcapsule contacting a plane, it is known that the force-displacement relationship of a sphere is not linear (Alves et al., 2015). Therefore a constitutive equation that includes this non-linearity along with viscous dissipation has been presented as

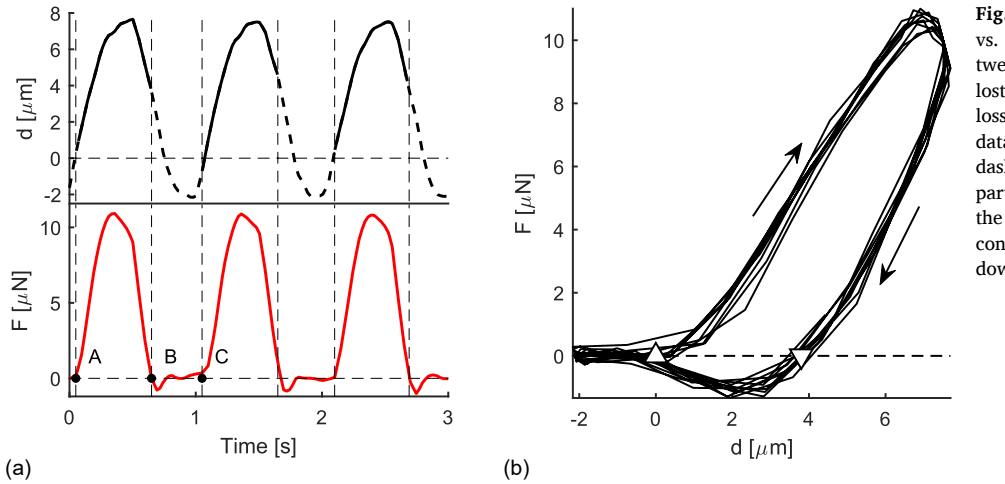

Fig. 5. (a) Example of position vs. time and force vs. time for a dynamic test in which contact between the rigid capillary and the microcapsule is lost. Note that the points of contact (**A and C**) and loss of contact (**B**) are labeled, and the position data in the loss of contact region is shown as a dashed lines. (b) Lissajous curve of the data in part (a). The direction of movement is shown by the arrows, and the points of contact and loss of contact are indicated by the upward (△) and downward triangles (▽).

follows:

$$F = Kd^n + \chi d^m \dot{d}. \tag{4}$$

here, F is the force, d is the deformation distance, and K and χ are model parameters related to contact stiffness and damping dissipation. For an elastic sphere, the power n is 1.5 in accordance with the Hertz model (Huang et al., 2021). As for the viscous term, researchers have proposed models with $m = 0.25$, 0.5, 1, and 1.5. Note, that this model reduces to the well-known Kelvin-Voigt model when $n = 1$ and $m = 0$, corresponding to a linear material.

To maintain consistency in the units, we made the *ad hoc* selection of $m = 0.5$ so that the relationship between the units of the two moduli ($[\chi] = [K]\cdot s$) is similar to that of elasticity and viscosity ($[\eta] = [E]\cdot s$):

$$F = Kd^{\frac{3}{2}} + \chi d^{\frac{1}{2}}\dot{d}. \tag{5}$$

This relationship can also be expressed in terms of stress and strain, where the storage and loss moduli have units of pressure:

$$\sigma = E'\varepsilon^{3/2} + (E''/\omega)\varepsilon^{1/2}\dot{\varepsilon}, \tag{6}$$

$$E' = \frac{K}{\sqrt{R}}; E'' = \frac{\omega\chi}{\sqrt{R}}. \tag{7}$$

here strain and stress, $\varepsilon = d/(2R)$ and $\sigma = F/R^2$, are defined with respect to the deformation d, the radius of the microcapsule R, and the force F; ω is the oscillation frequency. Note that to replace the viscous parameters (χ) with the loss moduli (E''), the inclusion of frequency (ω) is necessary to balance the units for the case when the deformation is sinusoidal.

To supplement the analysis of the data, we follow previous researchers by also visualizing the dynamic data as a "Lissajous plot" to describe qualitative aspects of the data (Yang et al., 2020; Mermet-Guyennet et al., 2014). Fig. 4 shows the Lissajous plots of data generated based on equation (4). Fig. 4 (b) and (c) correspond to a linear material, including the cases of purely elastic material (a straight line) and viscoelastic material (a closed loop). Note that for the curve of the viscoelastic case, the loop is symmetric about a straight line that passes through the origin and the center of the plot. Fig. 4(d) and (e) correspond to a nonlinear material (equation (5)) and in this case the profile is not symmetric.

3.5. Influence of aging on rheological properties

In the following sections, we discuss the rheological properties of the microcapsules and evaluate how they change with the age of a microcapsule. Fig. 6(a) shows example data for a microcapsule undergoing oscillatory compression. A phase shift between the force and displacement curve was observed, which indicates that the gellan gum microcapsules can be viscoelastic instead of being purely elastic. The same data is shown on a Lissajous plot in Fig. 6(b) and for the purposes of discussion we will show only Lissajous plots of the data in the remainder of the paper.

While testing different microcapsules at different ages, we noticed a range of different rheological behaviour. Fig. 6 shows representative data from the categories of data that we observed and these match the four different cases presented in section 3.4.3 and Fig. 4(b). This is interesting since it suggests that some of the microcapsules appear linear (i.e., match a Kelvin-Voigt model), while others exhibit a non-linear relationship between force and compression. However, if the compression amount is over a small enough distance (relative to the shape of the overall curve), even a non-linear function such as equation (6) can be approximated as linear. Also, at compressions further from the point of contact, the relationship between force and deformation for equation (6) appears more linear. Therefore, care must be exercised in selecting a model for analyzing the data and viewing the Lissajous plots can help in this process.

Aside from the four types of Lissajous plots in Fig. 6, we want to discuss the type of Lissajous plot shown in Fig. 5(b). While we mentioned that this type of profile indicates loss of contact during the oscillations, the presence of negative forces can result from adhesion forces between the microcapsule and compression plate (Sirghi, 2010). In this study, we also observed that aged microcapsules sometimes became sticky and stuck on the compression plate. However in most cases we believe that the negative forces measured are simply due to the hydrodynamic lubrication force (Leal, 2007) since we did not observe any negative

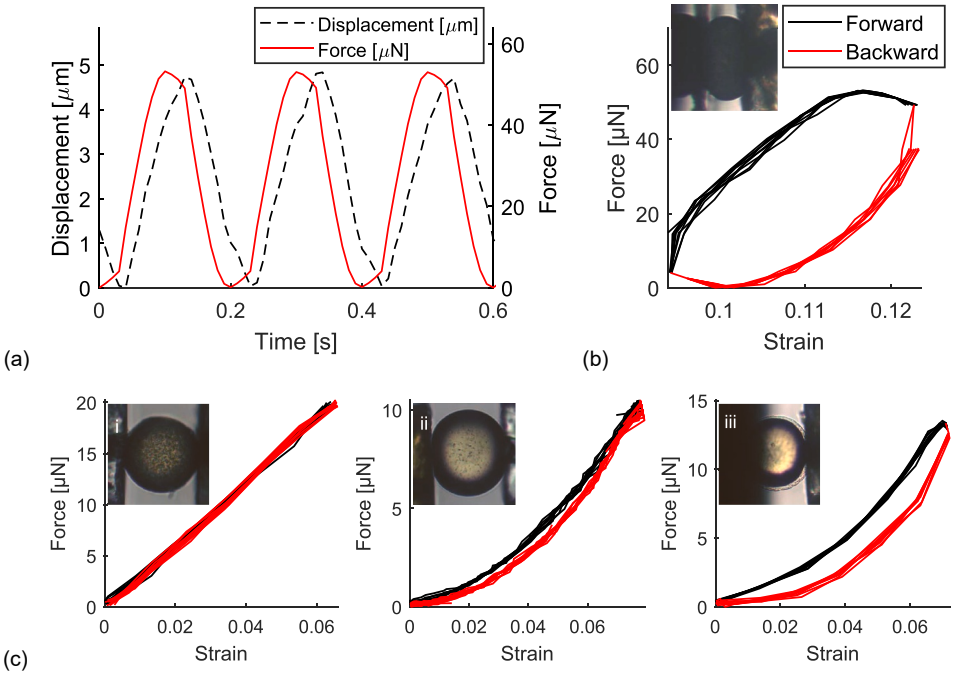

Fig. 6. (a) The position–time curve and force–time curve of a microcapsule from a dynamic measurement (capsule type: MTg). (b) Force-displacement profiles of four different aged microcapsules (i–iv: MtG, MTg, LTG, MTg; approximate age: 8 months) exhibit profiles resembling various models. Note that the force and strain are plotted relative to the minimum applied force and strain.

forces during the static compression tests. Regardless of the cause, the forces measured in this situation do not result from the microcapsule rheology.

With this in mind, in Fig. 7 we examine the Lissajous plots from three frequencies (0.01 Hz, 1.13 Hz, and 10 Hz) through the 8-day aging test. In this case, the profile of the Lissajous plots is more close to the nonlinear viscoelastic profile (Fig. 4(e)). For all frequencies, the overall slope of the Lissajous profile increased with the age of the microcapsule, indicating increased stiffness. This observation is consistent with the results of the elastic modulus test (Fig. 2(c)).

Further, at the lowest frequency (0.01 Hz), we see that the enclosed area between the compression and decompression curves increased with age. This suggests that the viscoelasticity of the microcapsule also increased with age. In terms of frequency dependence, the enclosed area decreases as frequency increases. Therefore, the elasticity of the microcapsule is more predominant at higher oscillation frequencies.

In addition, we note that some of the Lissajous plots contain regions with negative forces. As discussed before, this indicates a loss of contact. The loss of contact occurred at higher frequencies and higher ages of the microcapsule (Fig. 7, 1.13 and 10 Hz, day 4 and 6). Also, the depth of the "valley" (magnitude of the minimum force) increases with the oscillation frequency, which is consistent with a lubrication force. However, extracting information based on the position at which contact is lost is complicated by the irreversible deformation that occurs over time. Nevertheless, the fact that the curves are overlapping at each oscillation suggests that irreversible deformation is not playing a major role in an individual measurement.

Next, we extracted viscoelastic moduli from the dynamic tests to quantify the frequency dependence and the influence of aging. As discussed previously, there are multiple models that can potentially be used to describe the data and here we present an analysis of two representative sets of data, each using different values for the exponents in equation (4). The first set of data comes from a case where the Lissajous plot shows a nonlinear profile and we use equation (6) to extract the moduli. In Fig. 8(a) we plot E' and E'' vs. the oscillation frequency. We see that the storage modulus E' is essentially constant with frequency, while the loss modulus E' tends to decrease with frequency. This is consistent with our observation in Fig. 7, where the microcapsule becomes more elastic at higher frequencies.

The second set of data is from a measurement where the use of the linear version of equation (4) with $n = 1$ and $m = 0$ seems more appropriate. In this case, we found that both the storage modulus E' and the loss modulus E'' increase with the frequency. By examining the ratio between the two moduli E''/E', we found that the microcapsule becomes more viscous as the frequency increases, which is opposite from what we see in Fig. 8(a). One may attribute this difference in trends to the variety of complex behavior of that may be observed in these microcapsules. However, we also want to recall that the use of the linear version of the model is a potentially non-physical approximation, and it may not be appropriate to attempt to quantitatively compare the moduli extracted using different models.

To conclude this section, we also examine the data from the accelerated aging experiment. In Fig. 9 we plot the viscoelastic moduli at a frequency of 1 Hz as a function of the age of the microcapsule. As was found in the static tests, the storage modulus increases by about a factor of 40 over the 7 days. On the other hand, the loss modulus increased initially, but afterwards appeared to remain more-or-less constant. Finally, the loss modulus is consistently at least an order of magnitude smaller than the storage modulus which shows that the microcapsule is predominantly elastic throughout the aging process.

3.6. Cause of aging and implications for product applications

In the previous sections, we documented various changes in the properties of microcapsules as they age. Nevertheless, the mechanisms that cause aging in this case still require further investigation. We speculate that the cause of aging is either due to the reproduction of microorganisms within the core of the microcapsule, or to polymerization of the oil as it oxidizes. Since the solutions used to fabricate the microcapsules were not sterilized beforehand, the occurrence of microbial contamination is possible.

The hypothesis of microorganism reproduction is not inconsistent with many of our previous observations. For instance, we established that visual changes in the microcapsule appear to occur primarily in the core (vs. the shell). Also, gellan gum is sometimes used as a replacement for agar when culturing bacteria (McGuffey, 2018). The increased density of aged microcapsules could be related to the oil in the core being consumed and replaced with cells and waste products. Furthermore, the aging process occurred faster at room temperature than at 4C and there is no apparent trend between aging speed and capsule geometry. Finally, a core filled with microbial cells would be more stiff than a liquid core and subject to plastic deformation of the shape by rearrangement of the cells and/or extracellular matrix.

On the other hand, increases in opacity and density are consistent with polymerization due to oxidation of unsaturated fatty acids (Kalogianni et al., 2011). The observation of a spatially static structure within the core of the microcapsule, as described in section 3.3, may also be explained by the formation of a cross-linked network within this oil. Sunflower oil consists of approximately 90 wt% monounsaturated and polyunsaturated fatty acids, which are much more reactive with oxygen due to the carbon-carbon double bonds. However, whether the changing rheological properties are due to bacterial growth or polymerization, the spontaneous shedding of the shell of the microcapsule is likely due to some additional mechanism.

With the possible causes of aging in mind, we can foresee a few potential implications for product applications. Clearly, contamination due to microorganisms or oxidation of the oil (rancidity) will raise concerns around safety. Furthermore, even if the bacteria are not pathogenic they may degrade the active ingredients in the functional core (Pereira et al., 1998) and/or the integrity of the shell material (Hartemink et al., 1999). In addition to this, the changes in mechanical properties may also impact their performance. For example, the aged

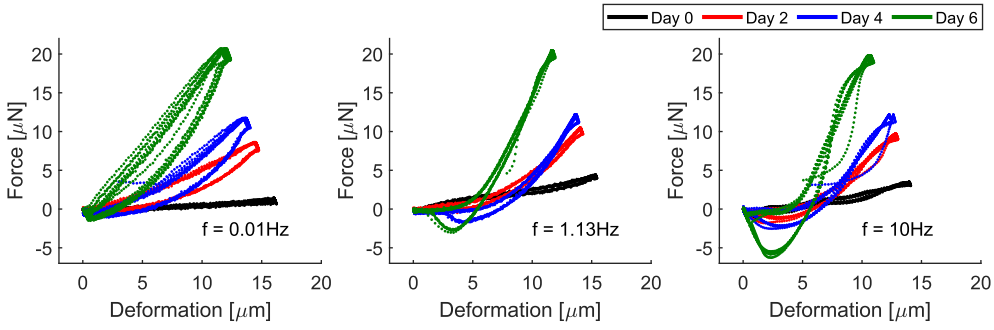

Fig. 7. Lissajous plots of selected frequencies (0.01, 1.13, and 10 Hz) and ages (0, 2, 4, 6 days) in the aging experiment through 8 days.

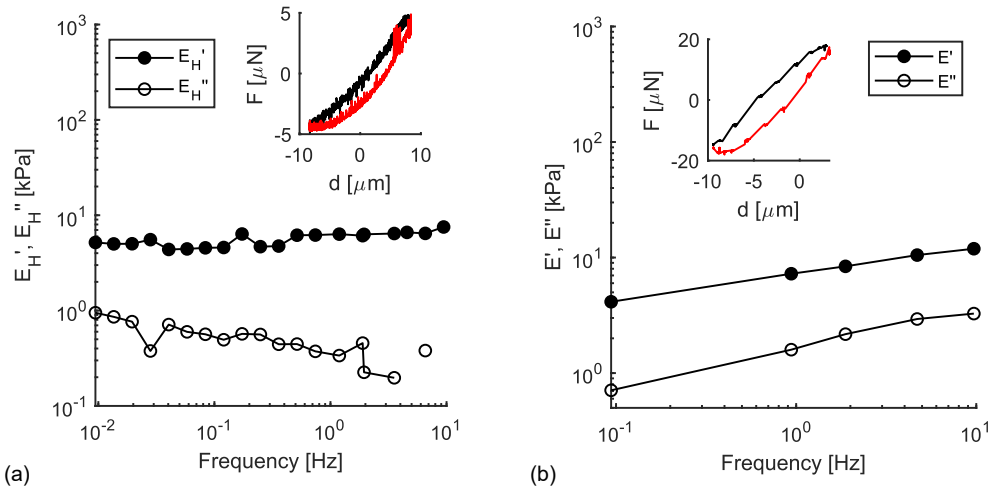

Fig. 8. The relationships between dynamic moduli and oscillation frequencies of two representative data sets. (a: Ltg, described by the viscoelastic Hertz model; b: MTg, described by the linear kelvin-Voigt).

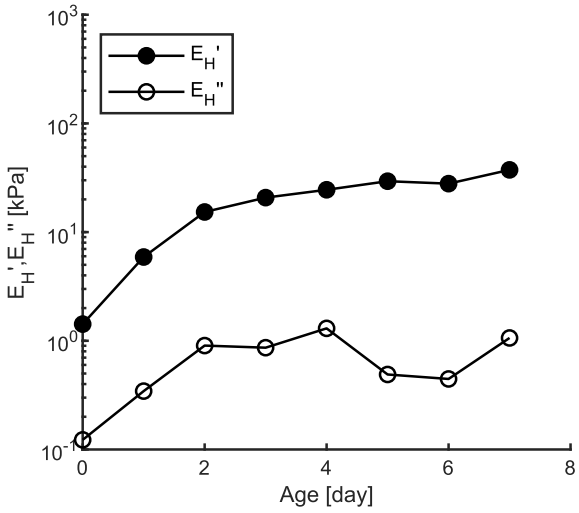

Fig. 9. Relationship between the dynamic moduli and the age of the microcapsule (1 Hz, strain = 0.05).

microcapsules are more likely to rupture which would reduce their effectiveness in sustained-release applications (Yan et al., 2019). Other negative consequences are also possible due to unwanted changes in mechanical properties, depending on how they have been tuned for a particular application.

4. Conclusions

In this paper, we examined the effects of aging on gellan gum microcapsules. We documented several outcomes including change in appearance, density, structure, and rheological properties. Each change represents a possible failure mode for these materials in a given application. We also identified several important considerations for method development when making rheological measurements on microcapsules. Specifically we show that effects due to backlash should be corrected in post-processing of rheological data and show that data should be ignored when loss of contact occurs due to viscoelasticity. In addition, we show that there is significant ambiguity in the selection of an appropriate constitutive model for extracting viscoelastic moduli from the measurements.

Our findings from the present rheological tests suggest that the rheological properties vary significantly with age and develop a complex frequency dependence. Furthermore, the aging of microcapsules was found to alter the properties of both the shell and the core. All of these changes that occur during aging are expected to have a significant, and largely negative, impact on any application they are used in. Some or all of the effects of aging observed here are likely to also occur in microcapsules made from other materials as well, therefore this work serves as a valuable reference point for future studies on aging of microcapsules.

Declaration of competing interest

There are no conflicts to declare.

Acknowledgements

We acknowledge the support of the Natural Sciences and Engineering Research Council of Canada (NSERC).

Appendix A. Supplementary data

Supplementary data to this article can be found online at https://doi.org/10.1016/j.foodhyd.2021.106982.

Author statement

Yun-Han Huang: Methodology, Software, Validation, Formal analysis, Investigation, Data Curation, Writing -Original Draft, Visualization, Xiran Li: Methodology, Investigation, Mariano Michelon: Conceptualization, Methodology, Resources, Bruna C. Leopercio: Conceptualization, Methodology, Resources, Marcio S. Carvalho: Conceptualization, Methodology, Resources, Writing -Review & Editing, Supervision, Project administration, Funding acquisition, John M. Frostad: Conceptualization, Methodology, Software, Validation, Writing -Review & Editing, Supervision, Project administration, Funding acquisition.

References

Alexandridou, S. (1995). On the synthesis of oil-containing microcapsules and their electrolytic codeposition. *Surface and coatings technology, 71*(3), 267–276. https://doi.org/10.1016/0257-8972(94)02322-H. Publisher: Elsevier.

Alizadegan, F., et al. (2017). Polyurethane-based microcapsules containing reactive isocyanate compounds: Study on preparation procedure and solvent replacement. *Colloids and surfaces A: Physicochemical and engineering aspects, 529*, 750–759. https://doi.org/10.1016/j.colsurfa.2017.06.058

Alves, J., et al. (2015). A comparative study of the viscoelastic constitutive models for frictionless contact interfaces in solids. *Mechanism and machine theory, 85*, 172–188. https://doi.org/10.1016/j.mechmachtheory.2014.11.020

Ashkin, A., Dziedzic, J. M., & Yamane, T. (1987). Optical trapping and manipulation of single cells using infrared laser beams. *Nature, 330*(6150), 769–771. https://doi.org/10.1038/330769a0. Number: 6150 Publisher: Nature Publishing Group.

Biviano, M. D., et al. (2021). Viscoelastic characterization of the crosslinking of lactoglobulin on emulsion drops via microcapsule compression and interfacial dilational and shear rheology. *Journal of colloid and interface science, 583*, 404–413. https://doi.org/10.1016/j.jcis.2020.09.008

Borgogna, M., et al. (2010). Food microencapsulation of bioactive compounds: Rheological and thermal characterisation of non-conventional gelling system. *Food chemistry, 122*(2), 416–423. https://doi.org/10.1016/j.foodchem.2009.07.043, 5th conference on water in food.

Caruso, M. M., et al. (2010). Robust, double-walled microcapsules for self-healing polymeric materials. *ACS applied materials & interfaces* (Vol. 2,(4), 1195–1199. https://doi.org/10.1021/am100084k. Publisher: American Chemical Society.

Chen, P. W., Erb, R. M., & Studart, A. R. (2012). Designer polymer-based microcapsules made using microfluidics. *Langmuir* (Vol. 28,(1), 144–152. https://doi.org/10.1021/la203088u

Fery, A., & Weinkamer, R. (2007). Mechanical properties of micro- and nanocapsules: Single-capsule measurements. *Polymer* (Vol. 48,(25), 7221–7235. https://doi.org/10.1016/j.polymer.2007.07.050

Frostad, J. M., et al. (2014b). Direct measurement of interaction forces between charged multilamellar vesicles. *Soft Matter, 10*(39), 7769–7780. https://doi.org/10.1039/.C3SM52785A

Frostad, J. M., Collins, M. C., & Leal, L. Gary (2013). Cantilevered-capillary force apparatus for measuring multiphase fluid interactions. *Langmuir* (Vol. 29,(15), 4715–4725. https://doi.org/10.1021/la304115k

Frostad, J. M., Collins, M. C., & Leal, L. Gary (2014a). *Direct measurement of the interaction of model food emulsion droplets adhering by arrested coalescence*.

Frostad, J. M., Paul, A., & Leal, L. Gary (2016). Coalescence of droplets due to a constant force interaction in a quiescent viscous fluid. *Physical review fluids* (Vol. 1)(3), Article 033904. https://doi.org/10.1103/PhysRevFluids.1.033904

Giménez-Ribes, G., Habibi, M., Leonard, M., & Sagis, C. (2020). Interfacial rheology and relaxation behavior of adsorption layers of the triterpenoid saponin Escin. *Journal of colloid and interface science* (Vol. 563,, 281–290. https://doi.org/10.1016/j.jcis.2019.12.053

Han, R., et al. (2019). Investigation on viscoelastic properties of urea-formaldehyde microcapsules by using nanoindentation. *Polymer testing* (Vol. 80), Article 106146. https://doi.org/10.1016/j.polymertesting.2019.106146

Hartemink, R., Schoustra, S. E., & Rombouts, F. M. (1999). Degradation of guar gum by intestinal bacteria. *Bioscience and microflora* (Vol. 18,(1), 17–25. https://doi.org/10.12938/bifidus1996.18.17

Y.-H. Huang et al. "Methods and models for the mechanical characterization of edible microcapsules". In: (2020). Under review by food hydrocolloids.

Huang, L., et al. (2019). Fabrication of multicore milli- and microcapsules for controlling hydrophobic drugs release using a facile approach. *Industrial & engineering chemistry research* (Vol. 58,(36), 17017–17026. https://doi.org/10.1021/acs.iecr.9b02351. Publisher: American Chemical Society.

Huang, Y.-H., et al. (2021). Models for the mechanical characterization of core-shell microcapsules under uniaxial deformation. *Food hydrocolloids.* , Article 106762. https://doi.org/10.1016/j.foodhyd.2021.106762

Kalogianni, E. P., Karapantsios, T. D., & Miller, R. (2011). Effect of repeated frying on the viscosity, density and dynamic interfacial tension of palm and olive oil". *Journal of food engineering* (Vol. 105,(1), 169–179. Publisher: Elsevier.

Kim, K., et al. (2008). Elastic and viscoelastic characterization of microcapsules for drug delivery using a force-feedback MEMS microgripper. *Biomedical microdevices* (Vol. 11,(2), 421. https://doi.org/10.1007/s10544-008-9248-6

Liu, X., et al. (2005). Multilayer microcapsules as anti-cancer drug delivery vehicle: Deposition, sustained release, and in vitro bioactivity. *Macromolecular bioscience* (Vol. 5,(12), 1209–1219. https://doi.org/10.1002/mabi.200500176

Leal, L. Gary (2007). *Advanced transport phenomena: Fluid mechanics and convective transport processes* (p. 933). Google-Books-ID: jbRGKo1IeOwC. Cambridge University Press.

Li, F., Wang, X., & Wu, D. (2015). Fabrication of multifunctional microcapsules containing n-eicosane core and zinc oxide shell for low-temperature energy storage, photocatalysis, and antibiosis. *Energy conversion and management* (Vol. 106,, 873–885. https://doi.org/10.1016/j.enconman.2015.10.026

Lulevich, Valentin V. (2003). Mechanical properties of polyelectrolyte microcapsules filled with a neutral polymer. *Macromolecules, 36*(8), 2832–2837.

Lulevich, V. V., et al. (2004). Investigation of molecular weight and aging effects on the stiffness of polyelectrolyte multilayer microcapsules. *Macromolecules, 37*(20), 7736–7741. Publisher: American Chemical Society.

Luo, W., et al. (2020). "Robust microcapsules with durable superhydrophobicity and superoleophilicity for efficient oil–water separation". *ACS applied materials & interfaces* (Vol. 12,(51), 57547–57559. https://doi.org/10.1021/acsami.0c15455. Publisher: American Chemical Society.

McGuffey, Jenna C. (2018). Bacterial production of gellan gum as a Do-It-Yourself alternative to Agar. *Journal of Microbiology & Biology Education, 19*(2).

Mercadé-Prieto, R., & Zhang, Z. (2012). Mechanical characterization of microspheres - capsules, cells and beads: A review. *Journal of microencapsulation* (Vol. 29,(3), 277–285. https://doi.org/10.3109/02652048.2011.646331

Mermet-Guyennet, M. R. B., et al. (2014). LAOS: The strain softening/strain hardening paradox. *Journal of rheology* (Vol. 59,(1), 21–32. https://doi.org/10.1122/1.4902000. Publisher: The Society of Rheology.

Michelon, M., Leopércio, B. C., & Carvalho, M. S. (2020). Microfluidic production of aqueous suspensions of gellan-based microcapsules containing hydrophobic compounds. *Chemical engineering science* (Vol. 211), Article 115314. https://doi.org/10.1016/.j.ces.2019.115314

do Nascimento, D. F., et al. (2017). Flow of tunable elastic microcapsules through constrictions. *Scientific reports* (Vol. 7,(1), 11898. https://doi.org/10.1038/s41598-01711950-2

Neubauer, M. P., Poehlmann, M., & Fery, A. (2014). Microcapsule mechanics: From stability to function. *Advances in colloid and interface science. Special issue: Helmuth möhwald honorary issue* (Vol. 207,, 65–80. https://doi.org/10.1016/j.cis.2013.11.016

Nitta, Y. (2005). Gelation and gel properties of gellan gum and xyloglucan. *Journal of Biological Macromolecules* (Vol. 5,(3), 47–52.

Okwara, C., et al. (2021). The mechanical properties of neurospheres. *Journal of advanced engineering materials*. https://doi.org/10.1002/adem.202100172

Ozkan, G., et al. (2019). A review of microencapsulation methods for food antioxidants: Principles, advantages, drawbacks and applications. *Food chemistry* (Vol. 272,, 494–506. https://doi.org/10.1016/j.foodchem.2018.07.205

Paulo, F., & Santos, L. (2017). Design of experiments for microencapsulation applications: A review. *Materials science and engineering: C* (Vol. 77,, 1327–1340. https://doi.org/10.1016/j.msec.2017.03.219

Pereira, M. Gloria, Mudge, S. M., & Latchford, John (1998). Bacterial degradation of vegetable oils. *Chemistry and ecology* (Vol. 14,(3), 291–303. Publisher: Taylor & Francis _eprint.

Sirghi, L. (2010). *Atomic Force Microscopy indentation of living cells* (Vol. 1).

Sliwka, W. (1975). Microencapsulation, 8. In *Angewandte chemie international edition in English* (Vol. 14, pp. 539–550). https://doi.org/10.1002/anie.197505391.

Suresh, S., et al. (2005). Connections between single-cell biomechanics and human disease states: Gastrointestinal cancer and malaria. *Acta biomaterialia* (Vol. 1,(1), 15–30. https://doi.org/10.1016/j.actbio.2004.09.001

Sworn, G., & Kasapis, S. (1998). Effect of conformation and molecular weight of co-solute on the mechanical properties of gellan gum gels. *Food hydrocolloids, 12*(3), 283–290. Publisher: Elsevier.

Tan, Y., et al. (2010). Mechanical characterization of human red blood cells under different osmotic conditions by robotic manipulation with optical tweezers. *IEEE transactions on biomedical engineering* (Vol. 57,(7), 1816–1825. https://doi.org/10.1109/.TBME.2010.2042448

Tatara, Y. (1991). On compression of rubber elastic sphere over a large range of displacements—Part 1: Theoretical study. *Journal of engineering materials and technology* (Vol. 113,(3), 285. https://doi.org/10.1115/1.2903407

Tatara, Y., Shima, S., & Lucero, J. C. (1991). On compression of rubber elastic sphere over a large range of displacements—Part 2: Comparison of theory and experiment. *Journal of engineering materials and technology* (Vol. 113,(3), 292–295. https://doi.org/10.1115/1.2903408

Utada, A. S., et al. (2005). Monodisperse double emulsions generated from a microcapillary device. *Science* (Vol. 308,(5721), 537–541. https://doi.org/10.1126/science.1109164

Verheyen, Connor A., et al. (2019). Characterization of polyethylene glycol–reinforced alginate microcapsules for mechanically stable cell immunoisolation. *Macromolecular Materials and Engineering, 304*(4), 1800679. https://doi.org/10.1002/mame.201800679. https://onlinelibrary.wiley.com/doi/pdf/10.1002/m

Wang, R., et al. (2011). Synthesis and characterization of chitosan/urea-formaldehyde shell microcapsules containing dicyclopentadiene. *Journal of applied polymer science* (Vol. 121,(4), 2202–2212. https://doi.org/10.1002/app.33829. https://onlinelibrary.wiley.com/doi/pdf/10.1002/app.33829

Wang, X.-Y., et al. (2020). Rheological behaviour of bitumen blending with self-healing microcapsule: Effects of physical and chemical interface structures. *Colloids and surfaces A: Physicochemical and engineering aspects* (Vol. 586), Article 124212. https://doi.org/10.1016/j.colsurfa.2019.124212

Yan, X., et al. (2019). Preparation and short-term aging properties of asphalt modified by novel sustained-release microcapsules containing rejuvenator. *Materials* (Vol. 12,(7), 1122. https://doi.org/10.3390/ma12071122. Number: 7 Publisher: Multidisciplinary Digital Publishing Institute.

Yang, F., et al. (2013). Preparation and evaluation of chitosan-calcium-gellan gum beads for controlled release of protein. *European food research and technology* (Vol. 237,(4), 467–479. https://doi.org/10.1007/s00217-013-2021-y

Yang, J., et al. (2020). Nonlinear interfacial rheology and atomic force microscopy of airwater interfaces stabilized by whey protein beads and their constituents. *Food hydrocolloids* (Vol. 101), Article 105466. https://doi.org/10.1016/j.foodhyd.2019.105466

Zhang, Z. (1999). Mechanical strength of single microcapsules determined by a novel micromanipulation technique". *Journal of microencapsulation* (Vol. 16,(1), 117–124. https://doi.org/10.1080/026520499289365

Zhang, Y.(张玉玲), et al. (2020). Dynamic mode of viscoelastic capsules in steady and oscillating shear flow. *Physics of fluids* (Vol. 32)(10), Article 103310. https://doi.org/10.1063/5.0023098. Publisher: American Institute of Physics.

Zhao, Q., et al. (2007). Hollow chitosan-alginate multilayer microcapsules as drug delivery vehicle: Doxorubicin loading and in vitro and in vivo studies. *Nanomedicine: Nanotechnology, biology and medicine* (Vol. 3,(1), 63–74. https://doi.org/10.1016/j.nano.2006.11.007